Development of Internet of Things (IoT)-Based Fish Dryer

Bless G. Ampuan [1,2*] and Vinyl H. Oquiño[2]
[1]Department of Electrical Engineering
University of Eastern Philippines
Catarman, Northern Samar, 6400 Philippines
[*]*bless.ampuan@uep.edu.ph*

[2]Graduate School
Eastern Visayas State University
Tacloban City, 6500 Philippines

Date received: August 29, 2025
Revision accepted: December 23, 2025

Abstract

This study presents the design and evaluation of an Internet of Things (IoT)-based fish dryer developed to improve traditional drying practices in Northern Samar, Philippines. The system integrates an ESP32 microcontroller for real-time monitoring and control of temperature, humidity, and weight using LCD and web-based interfaces. A bang–bang temperature controller with ±2°C hysteresis maintained stable drying conditions while preventing rapid switching. Drying trials of danggit (Siganus canaliculatus) reduced moisture content from 54–56 % to 24–29 % within 180–200 minutes, following a two-stage drying pattern of surface evaporation and diffusion. Univariate ANOVA revealed that drying location significantly affected temperature ($p < 0.001$, $\eta^2 = 0.771$) and humidity ($p < 0.001$, $\eta^2 = 0.578$), while drying duration showed no significant effect. The heat collector consistently exhibited the highest temperature and lowest humidity, confirming effective heat transfer and moisture control. The system achieved an average Specific Moisture Extraction Rate (SMER) of 0.0882 kg/kWh, demonstrating strong energy efficiency. Economic analysis indicated a 24.89 % return on investment and a payback period of 3.88 years. Overall, the IoT-based fish dryer proved technically efficient, energy-saving, and economically viable for small-scale fish processors.

Keywords: bang-bang temperature control, danggit *(Siganus canaliculatus)*, Internet of Things (IoT), fish drying technology, smart drying system

1. Introduction

The fishing industry remains a vital pillar of global food security and livelihoods, employing approximately 58.5 million people, most of whom are in Asia (Food & Agriculture Organization [FAO], 2020). In the Philippines, the fisheries sector significantly contributes to employment and the national economy, generating around 4.4 million metric tons of fish annually from commercial, municipal, and aquaculture sources (Philippine Statistics Authority [PSA], 2018; Statista, 2021; Food and Agriculture Organization of the United Nations [FAO], 2014). It plays a crucial role in supporting local incomes and nutrition (Philippine Statistics Authority [PSA], 2018; Bureau of Fisheries & Aquatic Resources [BFAR], 2017).

Fish remains an accessible and affordable source of dietary protein (Khan *et al*., 2021; Luthada-Raswiswi *et al*., 2021; Zhubi-Bakija *et al*., 2021; Gasco *et al*., 2020), especially for Filipinos, with dried fish serving as a staple component of the national diet (Ching *et al*., 2022; Department of Science and Technology–Food and Nutrition Research Institute [DOST-FNRI], 2020). However, fish is highly perishable, and traditional open-sun drying—while inexpensive and simple—remains the predominant preservation method (Venkateswarlu & Reddy, 2024; Fernandes & Tavares, 2024; Kong *et al*., 2024; Shimpy *et al*., 2023; Oria & Palconit, 2022; Bajet, Jr., 2013). This method, though widely practiced, is used to remove water from foods to preserve them (Venkateswarlu & Reddy, 2024; Perez *et al*., 2024; Oria & Palconit, 2022). However, it is often unhygienic, weather-dependent, and lacks environmental control, resulting in inconsistent product quality and postharvest losses (Venkateswarlu & Reddy, 2024; Fernandes & Tavares, 2024; Perez *et al*., 2024; Oria & Palconit, 2022; Solanki, 2020; Philippine Atmospheric, Geophysical and Astronomical Services Administration [PAGASA], 2021). Such challenges are particularly critical in humid, rainfall-prone coastal provinces like Northern Samar, where uncontrolled drying conditions exacerbate microbial spoilage and income instability (PAGASA, 2021).

To address these limitations, researchers have explored advanced drying technologies such as indirect solar dryers, hybrid solar–electric systems, and Internet of Things (IoT)-based monitoring frameworks (Venkateswarlu & Reddy, 2024; Perez *et al*., 2024; Jasmine & Triawati, 2022; Alvinika *et al*., 2021; Ilham *et al.,* 2021; Miano *et al*., 2023; Fernandes & Tavares, 2024; Jasmine & Triawati, 2022). IoT-enabled systems allow real-time monitoring and control of temperature, humidity, and mass, thereby improving drying uniformity and energy efficiency (Mishra *et al*., 2023; Ghafar *et al*., 2025). Nevertheless, most of these innovations remain costly, confined to laboratory-scale applications, or lack comprehensive technical and economic performance analyses—hindering their adoption among small-scale processors (Hasan *et al.,* 2025; Nnamchi *et al*., 2025; Hin *et al*., 2024; Oria & Palconit, 2022).

In response, this study aims to design, develop, and evaluate a low-cost IoT-based fish dryer capable of automated control and remote monitoring of temperature, humidity, and weight. The system is evaluated for its technical performance and economic feasibility relative to traditional drying methods (Reza & Hossain, 2024), providing a sustainable and scalable model for small-scale fish processors in Northern Samar and similar coastal communities (Deef *et al*., 2023; Younis *et al*., 2025).

2. Methodology

2.1 IoT-based Fish Dryer Components

The IoT-based fish dryer integrates multiple components to regulate temperature, humidity, and mass during drying, as shown in Figure 1. The system employs an ESP32 microcontroller with Wi-Fi connectivity for real-time monitoring and control (Mishra *et al*., 2023; Miano *et al*., 2023). Heating is provided by a 12 V DC, 150 W PTC resistive heater, protected by a 5 A thermal fuse and an inline circuit breaker (Venkateswarlu & Reddy, 2024; Deef *et al.*, 2023), while airflow is maintained by a 12 V DC axial fan (80 mm, 60 CFM) to ensure uniform circulation. The mass of the samples is monitored using four 5-kg load cells interfaced through an HX711 amplifier for real-time measurements (Yang *et al*., 2024; Ghafar *et al*., 2025). Three DHT22 temperature and humidity sensors (±0.5 °C, ±2 % RH accuracy) were calibrated using a reference digital hygrometer and a K-type thermocouple in a controlled environment chamber (Sulzer *et al*., 2022; Abdinoor *et al*., 2025). Sampling intervals were set at 10 minutes for mass and 30 minutes for temperature and humidity logging. All electrical wiring was shielded with 1.5 mm^2 copper wire, PVC-insulated, and enclosed in grounded metallic conduits, while Arduino-based firmware written in C++ was uploaded via the Arduino IDE. The combination of these components enables precise control of heat generation, airflow, and real-time monitoring of drying conditions throughout the drying process.

2.2 Design of the IoT-based Fish Dryer

2.2.1 Heat Collector and Drying Chamber

The energy required for moisture removal governs both the size and efficiency of solar dryers (Natarajan *et al*., 2022). In the IoT-based fish dryer, each drying batch processes 2 kg of fresh fish, wherein the moisture content is reduced from 54 % to 24 % on a wet basis. This reduction corresponds to approximately 0.789 kg mass (m) of water that must be evaporated per drying cycle.

Assuming the latent heat of vaporization of water (L_v) at 100°C is 2,260 kJ/kg, the theoretical energy requirement for moisture evaporation is calculated using Equation 1 (Gilago & Chandramohan, 2022).

$$Q_{required} = mL_v \tag{1}$$

Substituting the known values:

$$Q_{required} = 0.789kg \ x \ 2{,}260 \frac{kJ}{kg} = 1{,}782kJ$$

Converting to kilowatt-hours, the thermal energy required per batch is approximately 0.495 kWh, correcting the earlier overestimate of 49.57 kWh due to a unit conversion error. This revised value aligns with empirical energy consumption data for small-scale solar dryers handling similar loads (Natarajan *et al*., 2022; Chouikhi & Amer, 2023). Based on local solar data, Catarman, Northern Samar receives an average daily irradiation (G) of 9.7 kWh/m^2/day. Assuming the use of a flat-plate solar collector with thermal efficiency (η) of 75 %, the effective usable energy (Q_{usable}) is determined in Equation 2.

$$Q_{usable} = G_{\eta} \tag{2}$$

Substituting the known values:

$$Q_{usable} = 9.7x0.75 = 7.275kWh/m^2/day$$

This value represents the theoretical amount of solar energy absorbed by one square meter of collector area in a 2-hour window under average clear-sky conditions (Al Kindi *et al.*, 2023; Xu & Liu, 2025).

During a 2-hour drying operation, only a fraction of this daily insolation is available. Thus, the effective solar energy incident per square meter (Q_{usable}) during this period is $0.606\ kWh/m^2$.

To meet the total heat demand ($Q_{required}$) of 0.495 kWh per batch, the theoretical collector area (A_c) is computed using Equation 3.

$$A_c = \frac{Q_{required}}{Q_{usable}} \tag{3}$$

Substituting the known values:

$$A_c = \frac{0.495}{0.606} = 0.817m^2$$

Under ideal conditions, a collector area of ~0.82 m^2 can supply enough thermal energy to evaporate the required moisture in two hours. In practice, heat losses from conduction, convection, imperfect insulation, and the energy needed to heat the fish and chamber air reduce efficiency (Zaboli *et al.*, 2023). Accounting for a realistic overall system efficiency (η) of 60 %, the required collector area ($A_{realisitic}$) increases using Equation 4.

$$A_{realisitic} = \frac{A_C}{\eta} \tag{4}$$

Substituting the known values:

$$A_{realisitic} = \frac{0.817}{0.6} = 1.36m^2$$

Thus, a solar collector area between 1.3 and 1.5 m^2 is technically sufficient to sustain a 2-hour drying cycle for 2 kilograms of fish under Catarman's solar conditions (Gilago & Chandramohan, 2022; Al Kindi *et al.*, 2023).

The drying chamber as shown in Figure 1, was designed for 35 danggit fish, each averaging 0.00015 m^3 (Bureau of Agriculture and Fisheries Product Standards [PNS/BAFPS 68:2008], 2008). Two 0.8 × 0.8 m trays, each holding

25 fish, provide a total drying area of 1.28 m^2. Allowing 10 % extra for airflow, the chamber cross-sectional area is ~1.41 m^2, with a depth of 0.4 m, giving a total volume of 0.56 m^3. Vertical spacing accounts for tray thickness (0.025 m) and divides the remaining 0.35 m into three ~0.12 m segments (below, between, and above trays) to ensure uniform airflow for efficient drying (Chouikhi & Amer, 2023; Xu & Liu, 2025; Natarajan *et al.,* 2022).

Figure 1. IoT-based fish dryer

2.2.3 System Schematics

Figure 2 shows the actual circuit and designed schematics of the system, respectively. It is powered by a 230 AC source. A Power Supply converts 230 AC to 12 V DC for the 12V loads such as the exhaust fan, blowing fan and heating element. A 12 V DC to 5 V DC Buck Converter is acquired to convert 12V voltage to 5V to power up the ESp32 microcontroller. The ESp32 controlled the three (3) DHT22 sensors, an H×711 weight sensor with 4 load cells, a 2×16 LCD, two (2) push button switches, 4-relay Module, exhaust fan, blowing fan, and heating elements. The 4-relay Module serves as the electronic switches of the electrical devices such as the exhaust fan, blowing fan and heating element. Several researchers utilized the above-mentioned components (Hasan *et al.*, 2025; Ampuan, 2025; Ampuan *et al.*, 2025; Dasmen & Haq, 2023; Jasmine & Triawati, 2022; Ilham *et al.,* 2021; Alvinika *et al.*, 2021; Tolentino *et al.*, 2021).

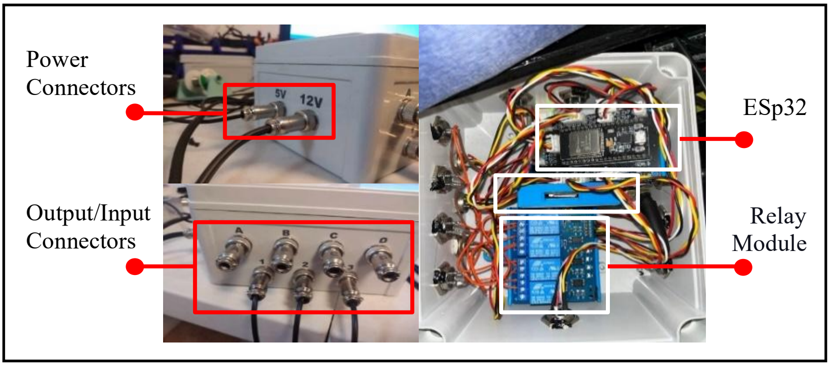

Figure 2. Circuit connection of the system

2.2.4 Safety and Electrical Compliance Considerations

For potential commercial deployment, the IoT-based fish dryer was designed following the Philippine Electrical Code (Institute of Integrated Electrical Engineers of the Philippines Inc. [IIEE], 2017) and relevant IEC low-voltage standards. All circuits operate at 12 V DC, with the 12 V, 150 W PTC heater protected by thermal cutout and fuse isolation, and wiring enclosed in insulated panels with heat-resistant conduits. The ESP32 controller and sensors are isolated via relays rated at twice the heater current, with a 5 A main fuse and reverse-polarity protection. Future commercial versions may include RCDs and IEC 60335/60529 compliance testing, ensuring safe operation in humid drying environments.

2.2.5 Modes of System Peration

Operational modes of the dryer are illustrated in Figure 3 and include initialization, calibration, drying, and reset cycles. The system employs a bang–bang control strategy, in which the heater operates fully ON or OFF based on sensor readings (Hammer, 2024; Amigues *et al*., 2023). When the drying chamber temperature falls below the lower limit, the heater switches ON, and when the temperature exceeds the upper limit, the heater switches OFF. A hysteresis of ±2 °C prevents rapid cycling, while a 30-second delay between successive switching events reduces relay wear and prolongs component life. This control strategy ensures that the drying temperature remains stable within the optimal range, minimizing energy consumption and maintaining product quality.

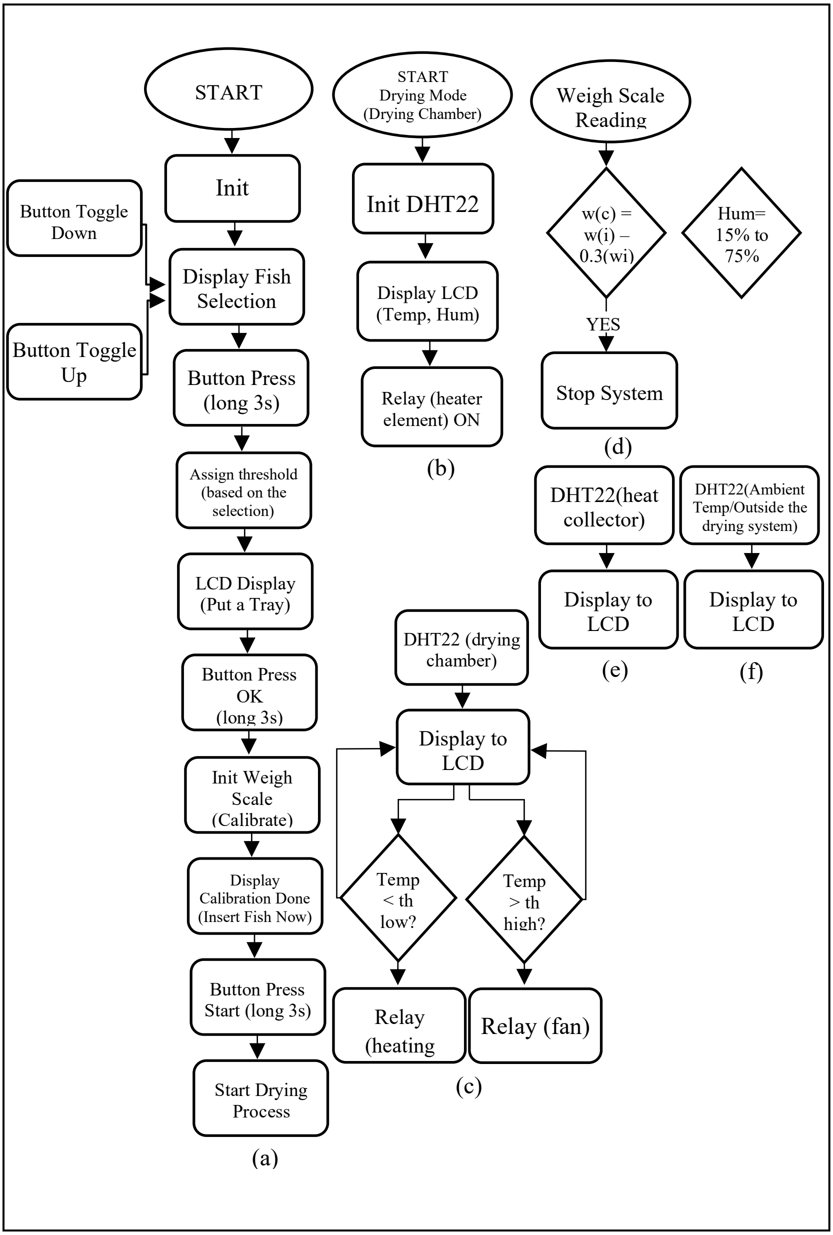

Figure 3. Operational Flow chart of the system: initialization (a), drying mode (b), chamber monitoring (c), mass monitoring (d), collector monitoring (e), and ambient monitoring (f)

2.2.6 Monitoring and Data Logging

Remote monitoring is achieved through LCD display and IoT web server interfaces as shown in Figure 4, recording temperature, humidity, and sample mass. Data acquisition followed the sensor types and logging intervals described in Section 2.1, enabling real-time tracking and historical data analysis for each drying trial.

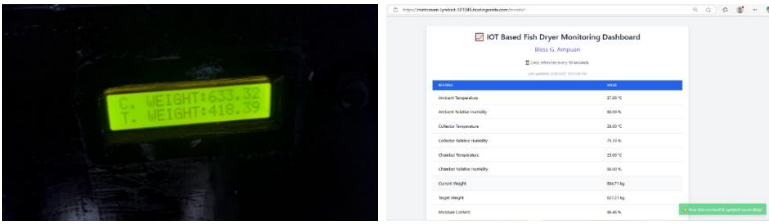

(a) (b)

Figure 4. Remote monitoring: LCD display (a), and IoT-based (b)

2.3 Design Equations

The determination of moisture removal, M_w, of the fish samples was calculated using Equation 5 (Taide & Deshmukh, 2018; Mehta *et al*., 2018).

$$M_w = \frac{M_p\ (M_i - M_f)}{100 - M_f} \tag{5}$$

where M_p is the initial mass of product to be dried in kg; M_i= the initial moisture content; M_f is the final moisture content.

The moisture content (wet basis), $\%\ w.b.$, was calculated using Equation 6, which has been widely used in drying studies (Dasin *et al*., 2019; Taide & Deshmukh, 2018; Mehta *et al*., 2018).

$$\%\ w.b. = \frac{m_i - m_f}{m_i}\ x\ 100 \tag{6}$$

where M_i= the initial moisture content (*%w.b.*); M_f is the final moisture content.

The drying rate, D, was calculated using Equation 7, as described by various researchers (Guanco & Casinillo, 2021; Dasin *et al*., 2019; Taide & Deshmukh, 2018).

$$D = \frac{m_i - m_f}{t_d} \tag{7}$$

where m_f is the final mass of the sample or dried fish (kg); m_i is the initial mass of the sample or fresh fish (kg); t_d= drying time (h).

2.4 Experimental Procedure

Fresh danggit *(Siganus canaliculatus)* fish were sourced from a single catch to ensure uniform size and moisture content. Fish were brined in a 20–25 % salt solution for 1 hour, drained, and air-dried for 10 minutes before loading. Drying trials were conducted under the conditions described in Section 2.1, with three independent trials and two replicate trays per trial to ensure reliability. Individual fish were randomly assigned to trays to minimize positional bias. Average values of drying rate, temperature, and final moisture content were calculated across replicates.

2.5 Data Acquisition and Analysis

Data were collected using IoT sensors and validated with calibrated instruments. Temperature and humidity were recorded every 30 min, and sample weight every 10 min to compute moisture content from weight loss. Two replicate trays per trial and three independent trials ensured reliability, with mean values used to assess drying performance. Energy consumption was measured by the system, theoretical requirements were estimated from literature, and data were analyzed in Microsoft Excel using descriptive statistics.

2.6 Data Analysis

IoT sensors recorded temperature, humidity, and sample mass, validated using calibrated instruments. Energy consumption was measured and compared with theoretical estimates derived from the design equations. Descriptive statistics and graphical analyses were performed in Microsoft Excel. Inferential analysis using Univariate ANOVA (IBM SPSS Statistics, Version 29) evaluated the effects of drying duration and other factors on air temperature and humidity. Results included F-values, p-values, and partial η^2

to quantify effect sizes. Temperature regulation was verified through heater ON–OFF patterns and bang–bang control performance. Economic assessment, including payback period and ROI, followed Bajet, Jr. (2013).

3. Results and Discussion

3.1 Profile of Traditional Sun Drying

3.1.1 Drying Capacity

The fresh danggit *(Siganus canaliculatus)* batches averaged 6-23 kg (overall average 13.5 kg). Brining reduced the mass to 53-55 % of the fresh weight, and drying further reduced it by 30 % of the brined weight. Brine salting is one of the oldest, most traditional, and economically viable methods for preserving edible animal proteins (Mebratu *et al.*, 2024; Gasco *et al.*, 2020; Binici & Kaya, 2018). Fresh danggit *(S. canaliculatus)* batch sizes vary, averaging 13.5 kg. Brining causes a significant weight loss (around 45-47 %), and drying leads to another 30 % reduction from the brined weight. This data is key for yield estimation and understanding mass changes during danggit processing.

3.1.2 Drying Duration, Moisture Content Reduction, and Drying Rate

Results indicate that the average drying duration for danggit *(S. canaliculatus)*, considering both good and bad weather, is approximately 3 days, reflecting the long drying process as one of the reported major problems of the traditional sun drying from the fish processors – the weather dependence. Several studies have shown that it usually takes 3 to 7 days, or longer if insufficient light is available (Natarjan *et al.*, 2022; Hasan *et al.*, 2025). Findings of the preliminary survey revealed that an average moisture content reduction of dried danggit is around 30 % from brining.

3.1.3 Drying Temperature and Relative Humidity

The drying temperature is dependent only on the ambient temperature produced by the sun. The researcher gathered data through the PAGASA to accumulate the average ambient temperature and relative humidity in the nearest station, which is Catarman. Based on the available data from 2018 to

2022, the annual minimum and maximum ambient temperatures are 24°C and 31°C, respectively, while the minimum and maximum relative humidity are 78 % and 92 %, respectively, with an average relative humidity of around 86 %.

3.2 Performance of the IoT-based Fish Dryer

Due to environmental and logistical constraints, parallel experiments under identical ambient conditions were not feasible. Instead, comparative data from local traditional sun-drying operations and PAGASA ambient records were used to normalize conditions, consistent with field-based solar drying studies (Younis *et al*., 2025; Fernandes & Tavares, 2024). This approach enabled relative performance evaluation despite the lack of fully controlled conditions.

3.2.1 Mass Reduction Rate

Figure 5 shows the mass of danggit (*S. canaliculatus*) decreased rapidly during the initial drying stage and more slowly thereafter, reflecting the typical transition from free moisture removal to diffusion-limited bound water loss (Babalis & Belessiotis, 2006; Schlünder, 1988). Differences among trials indicate the effects of loading and airflow distribution, where lighter loads enhanced mass transfer and heavier loads restricted circulation, consistent with prior fish and solar-assisted drying studies (Shimpy *et al*., 2023; Nnamchi *et al*., 2025; Wang *et al*., 2024). Overall, the results demonstrate stable and controlled drying performance of the IoT-based system, consistent with established drying kinetics and hybrid drying principles (Hasan *et al*., 2025).

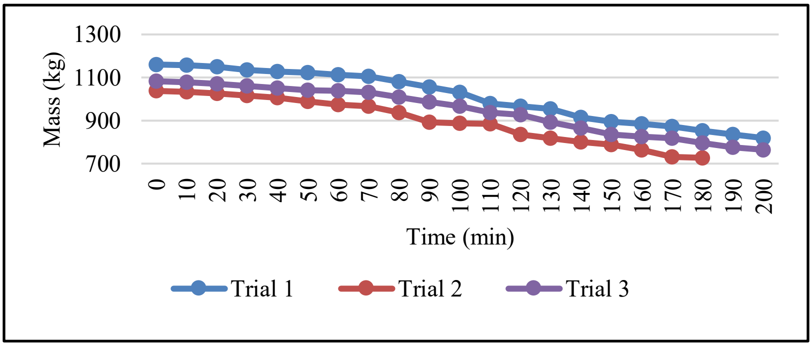

Figure 5. Instantaneous average mass reduction

3.2.2 Moisture Content Reduction Rate

Figure 6 shows the typical thin-layer drying behavior of danggit (*S. canaliculatus*) across the three trials. All trials exhibited a rapid initial moisture loss during the first stage, followed by a slower decline, reflecting surface moisture evaporation and subsequent diffusion-controlled removal of bound water (Babalis & Belessiotis, 2006; Wang *et al*., 2024; Hasan *et al*., 2025; Nnamchi *et al*., 2025). Differences among trials highlight the effects of loading density, airflow uniformity, and thermal distribution. Lower loading improved moisture removal rates and drying uniformity, while higher loading slightly reduced drying efficiency, consistent with previous studies on fish and aquatic product drying (Shimpy *et al*., 2023; Wang *et al*., 2024; Fernandes & Tavares, 2024). Overall, the observed trends confirm that the IoT-based dryer reproduces the multi-stage drying kinetics characteristic of convective and solar-assisted systems, achieving efficient surface evaporation followed by internal moisture diffusion.

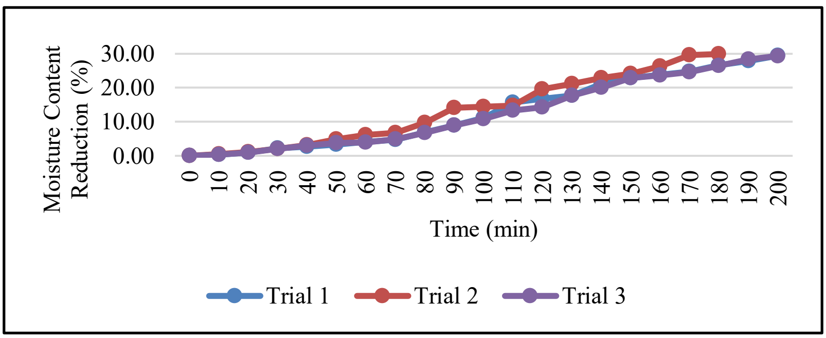

Figure 6. Instantaneous average moisture content reduction

3.2.3 Drying Rate

Figure 7 shows the drying rate of danggit (*S. canaliculatus*) across the three trials. All trials exhibited a typical pattern with an initial acceleration phase, followed by a nearly constant-rate period. The early stage reflects surface water evaporation, while the later constant-rate period indicates a transition to diffusion-controlled drying, where internal moisture migrates to the surface before evaporating (Schlünder, 1988; Babalis & Belessiotis, 2006; Wang *et al*., 2024). Differences among trials highlight the effect of loading density and airflow. Lower loading improved air circulation and heat transfer, resulting in faster drying rates, whereas higher loading restricted airflow and slowed moisture removal. Intermediate loading produced moderate drying efficiency, confirming the importance of proper load optimization in small-scale dryers (Nnamchi *et al.*, 2025; Shimpy *et al.*, 2023). Overall, the drying rate trends confirm that the IoT-based dryer maintains consistent and controlled drying behavior, comparable to established convective and hybrid drying systems.

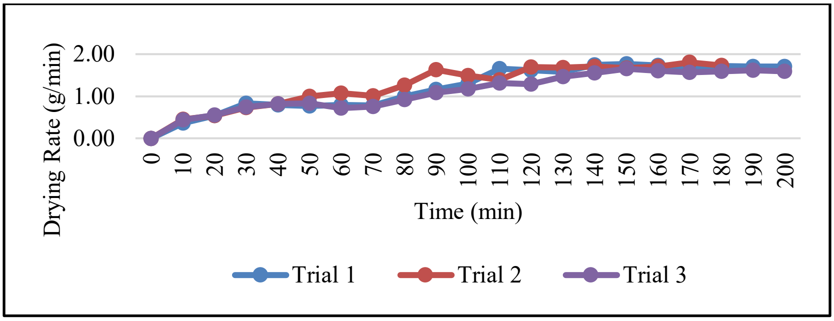

Figure 7. Instantaneous average drying rate

3.2.4 Energy Efficiency

Table 1 presents the specific moisture retraction rate of the IoT-based fish dryer. Across three trials, the IoT-based fish dryer demonstrated consistent performance with low variability in measured parameters. The mass of moisture removed averaged 0.314 ± 0.042 kg, while the Specific Moisture Extraction Rate (SMER) was 0.088 ± 0.007 kg/kWh (CV ≈ 8.4 %), indicating good repeatability. Energy consumption (3.54 ± 0.21 kWh) and drying duration (3.22 ± 0.19 h) were also stable, reflecting consistent heater operation and airflow. These results confirm that the dryer maintains nearly uniform energy efficiency and operates reliably within typical ranges for small-scale electric dryers (0.05–0.1 kg/kWh), with potential improvements in air distribution and heater control to further enhance performance (Gilago & Chandramohan, 2022).

Table 1. Specific moisture retraction rate of the IoT-based fish dryer

Indicators	Trial 1	Trial 2	Trial 3	Mean	Standard Deviation
Initial Mass (kg)	1.1603	1.0377	1.0826	1.0935	0.0620
Initial Moisture Content (%)	55.7	53.9	54.8	54.8	0.90
Final Moisture Content (%)	25.6	28.2	24.9	26.23	1.74
Mass of moisture removed (kg)	0.3493	0.2677	0.3237	0.3136	0.0417
Power consumed (kW)	1.1	1.1	1.1	1.10	0.00
Drying duration (hr)	3.33	3	3.33	3.22	0.19
Energy Consumed (kWh)	3.66	3.3	3.66	3.54	0.21
Specific Moisture Extraction Rate (kg/kWh)	0.0954	0.0808	0.0885	0.0882	0.0074

3.2.5 Air Temperature and Relative Humidity Monitoring

Figures 8–10 show the air temperature and relative humidity inside the drying chamber during the three trials. Across all runs, an inverse relationship was observed: as temperature increased, relative humidity decreased, reflecting an effective heat collector and ventilation system that supports continuous moisture removal (Hasan *et al*., 2025; Ruzikulov *et al*., 2023).

A transient humidity spike occurred in Trial 3 despite relatively stable temperatures. Possible causes include sudden ambient temperature fluctuations, temporary fan speed reductions, or slight decreases in solar collector efficiency. Similar short-term variations have been reported in other IoT-assisted drying systems, which are quickly corrected through automated feedback control (Wang *et al*., 2024; Shimpy *et al*., 2023; Nnamchi *et al*., 2025). The system's rapid recovery highlights the robustness of the IoT-based control; though additional redundancy or humidity-based alarms could further stabilize performance.

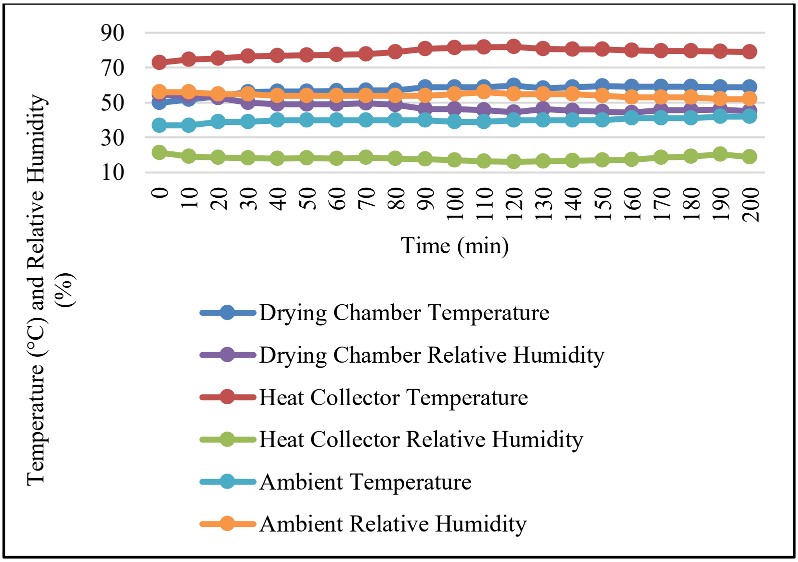

Figure 8. Average drying temperature and relative humidity monitoring (first trial)

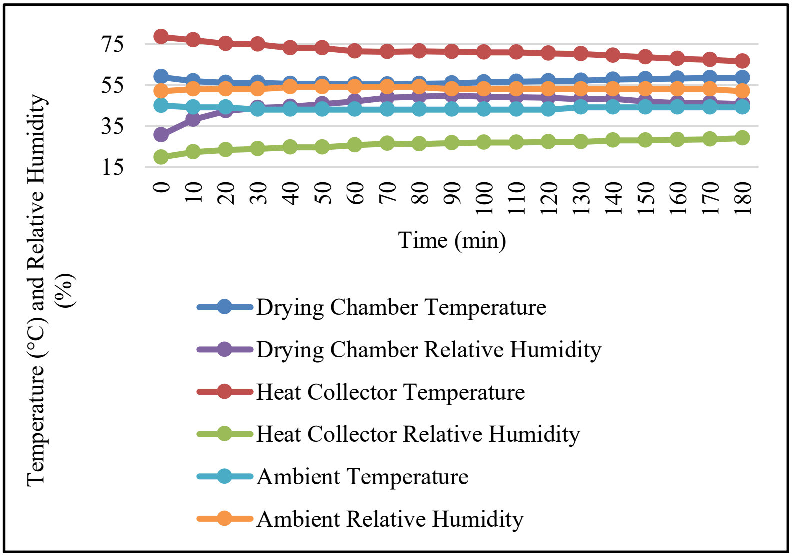

Figure 9. Average drying temperature and relative humidity monitoring (second trial)

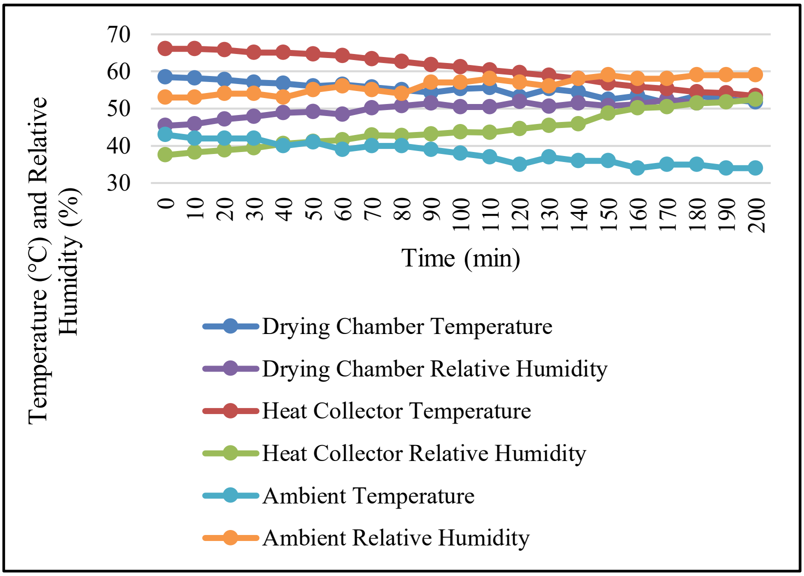

Figure 10. Average drying temperature and relative humidity monitoring (third trial)

3.2.6 Effect of Drying Duration and Reduction Parameters on Drying Performance

Univariate ANOVA (Table 2) showed significant effects of drying duration ($F(17,108) = 3.36$, $p < 0.001$, $\eta^2 = 0.346$), reduction rate type ($F(2,108) = 8285.59$, $p < 0.001$, $\eta^2 = 0.994$), and their interaction ($F(34,108) = 4.55$, $p < 0.001$, $\eta^2 = 0.589$). Large effect sizes indicate that both time and parameter type strongly influence drying performance, with rate type explaining nearly all variation.

Significant duration effects confirm that the IoT-based control algorithm effectively regulated heat and airflow, maintaining stable drying kinetics. Interaction effects suggest parameters responded differently over time, with moisture content and drying rates peaking mid-process and slowing as bound water dominated, consistent with the transition from constant-rate to falling-rate periods (Erbay & Icier, 2010). The high adjusted R^2 (0.990) indicates the model reliably explains variation, demonstrating the dryer's capacity for optimized, sensor-driven operation and potential for adaptive, real-time control.

Table 2. Univariate ANOVA results showing significant main and interaction effects of drying duration and reduction parameters on drying performance

Source	SS	df	MS	F	η²
Corrected Model	32027700.19[a]	53	604296.23	316.66	.994
Intercept	16487649.07	1	16487649.07	8639.71	.988
Drying Duration	109098.83	17	6417.58	3.363	.346
Reduction Rates	31623714.141	2	15811857.07	8285.59	.994
Drying Duration*Reduction Rates	294887.225	34	8673.15	4.55	.589
Error	206102.524	108	1908.36		
Total	48721451.779	162			
Corrected Total	32233802.714	161			

Note: a. R Squared = .994 (Adjusted R Squared = .990). Partial η² (eta squared) represents effect size. All p-values <.001.

Figure 11 illustrates the drying behavior of danggit (*S. canaliculatus*) through drying rate, moisture content reduction, and mass reduction over time. The drying rate and moisture content reduction increased during the initial phase and plateaued around 150 minutes, while mass reduction gradually declined throughout the process. This pattern reflects typical drying kinetics of biological materials, with surface water evaporation dominating early and internal diffusion controlling the later falling-rate period. Stabilization after 150 minutes indicates that the product approached equilibrium moisture, suggesting optimal drying conditions were achieved.

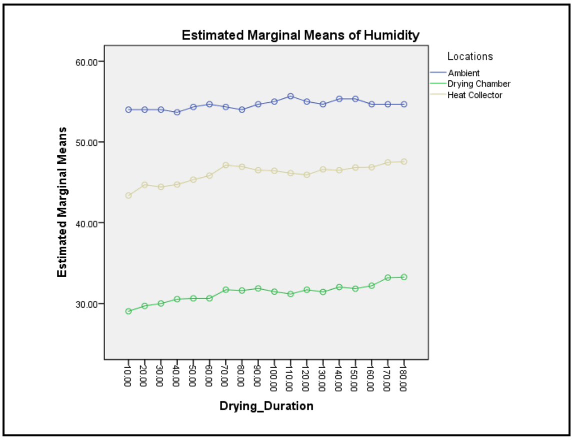

Figure 11. Variation of drying rate, moisture content reduction, and mass reduction with respect to drying duration

3.2.7 Analysis of Air Temperature Variation Across Drying Duration and Locations

Univariate ANOVA (Table 3) examined the effects of drying duration and location (ambient, drying chamber, heat collector) on air temperature. Location had a highly significant effect ($F(2,108) = 181.85$, $p < 0.001$, $\eta^2 = 0.771$), while drying duration ($F(17,108) = 0.061$, $p = 1.000$, $\eta^2 = 0.010$) and the interaction between duration and location ($F(34,108) = 0.016$, $p = 1.000$, $\eta^2 = 0.005$) were not significant, indicating stable temperatures over time and consistent spatial patterns.

The high η^2 for location and strong model fit ($R^2 = 0.772$, Adjusted $R^2 = 0.660$) show that ~77 % of temperature variance was explained by measurement location. The drying chamber exhibited the highest mean temperature, followed by the heat collector and ambient air, reflecting efficient thermal transfer. These results confirm that the IoT-controlled system maintained stable, uniform thermal conditions, essential for consistent moisture removal and product quality.

Table 3. Univariate ANOVA results for the effects of drying duration and location on air temperature

Source	SS	df	MS	F	η^2
Corrected Model	21746.088[a]	53	410.304	6.892	.772
Intercept	504019.156	1	504019.156	8466.000	.987
Drying Duration	61.794	17	3.635	.061	.010
Reduction Rates	21652.641	2	10826.320	181.850	.771
Drying Duration*Locations	31.652	34	.931	.016	.005
Error	6429.727	108	59.535		
Total	532194.970	162			
Corrected Total	28175.814	161			

Note: a. R Squared = .772 (Adjusted R Squared = .660). Partial η^2 (eta squared) represents effect size. All p-values <.001.

Figure 12 shows the estimated marginal means of air temperature across drying duration for the heat collector, drying chamber, and ambient environment. Temperature remained relatively stable throughout the process, with the heat collector consistently the hottest, the drying chamber intermediate, and ambient air the coolest. The clear separation among the temperature profiles indicates an effective thermal gradient from the collector to the chamber, ensuring efficient heat transfer while maintaining environmental isolation. The minimal fluctuations over time reflect thermal stability, supporting consistent drying rates and preventing overheating of the fish samples.

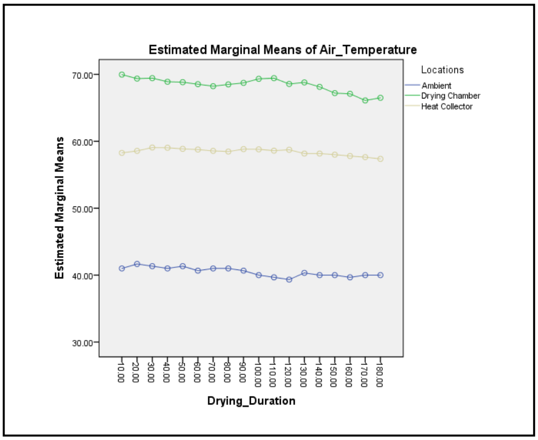

Figure 12. Variation of air temperature across drying durations and locations

3.2.8 Analysis of Relative Humidity Variation Across Drying Duration and Locations

Univariate ANOVA (Table 4) showed a significant effect of location on humidity ($F = 73.851$, $p < 0.001$, partial $\eta^2 = 0.578$), while drying duration ($F = 0.063$, $p = 1.000$) and the interaction between duration and location ($F = 0.010$, $p = 1.000$) were not significant. This indicates that humidity differed among ambient, drying chamber, and heat collector zones but remained largely stable over time within each zone. The results suggest that the dryer's design effectively isolates each zone, with ambient air maintaining higher humidity, the drying chamber moderately reduced due to active airflow and heating, and the heat collector the lowest, reflecting efficient moisture evacuation. The large effect size highlights the role of spatial factors in controlling humidity and confirms that the system maintains stable microclimatic conditions essential for uniform drying and prevention of surface hardening. Overall, humidity distribution is primarily governed by location rather than time, demonstrating effective moisture management and functional separation of zones in the IoT-based dryer.

Table 4. Univariate ANOVA results for the effects of drying duration and location on relative humidity

Source	SS	df	MS	F	η²
Corrected Model	15099.143[a]	53	284.889	2.814	.000
Intercept	313623.200	1	313623.200	3097.511	.000
Drying Duration	109.285	17	6.429	.063	1.000
Reduction Rates	14954.845	2	7477.422	73.851	.000
Drying Duration*Locations	35.013	34	1.030	.010	1.000
Error	10935.007	108	101.250		
Total	339657.350	162			
Corrected Total	26034.150	161			

Note: a. R Squared = .580 (Adjusted R Squared = .374). Partial η² (eta squared) represents effect size. All p-values <.001.

Figure 13 shows the estimated marginal means of humidity for the ambient, drying chamber, and heat collector zones throughout the drying duration. Humidity remained stable over time within each zone, with the ambient environment highest, the drying chamber intermediate, and the heat collector lowest. The steady separation among zones indicates a well-regulated moisture gradient, facilitating efficient heat absorption in the collector and uniform drying in the chamber. These trends are consistent with the ANOVA results (Table 4), where location significantly affected humidity ($F = 73.851$, $p < 0.001$, partial $\eta^2 = 0.578$), while drying duration and its interaction with location were not significant. Overall, the IoT-based dryer effectively maintains spatially controlled humidity, ensuring consistent moisture removal and preventing over-drying or spoilage of the fish.

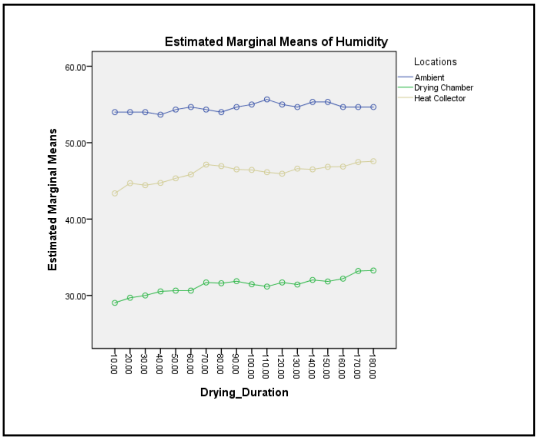

Figure 13. Variation of relative humidity across drying durations and locations

3.3 Projected Economy of the IoT-based Fish Dryer

3.3.1 Financial Operation Indicators

Table 5 compares the operational and financial performance of traditional and IoT-based fish drying systems. The traditional method operates seasonally for seven months, involves long drying times per batch, and requires continuous manual labor for handling, monitoring, and protection of fish. In contrast, the IoT-based dryer enables year-round operation, shorter batch durations, and automated control of temperature and airflow, substantially reducing routine labor requirements rather than eliminating them entirely.

While the IoT-based system still requires human involvement for loading and unloading, periodic supervision, maintenance, and system management, the intensity and frequency of labor are significantly lower than in traditional sun drying. These operational improvements translate into higher production throughput and revenue despite smaller batch sizes. Although the IoT-based dryer incurs energy and maintenance costs, these are largely offset by reduced labor input, improved process consistency, and increased productivity. Overall, the IoT-based fish dryer demonstrates enhanced operational efficiency and economic potential relative to conventional drying practices.

Table 5. Annual financial and performance operation indicators of traditional and IoT-based fish drying systems

Indicators	Traditional	IoT-based
Operation Period		
No. of operation months per year	7 months	12 months
Average drying duration per batch	72 hours	16.6 hours
Total monthly active drying duration	84hrs	197.5 hours
Average capacity of fresh fish per batch	15kg	2kg
Production Capacity (Monthly basis)		
No. of drying batches per month	12 batches	72 batches
Total fresh *danggit* processed per month	180kg	216 kg
Total dried *danggit* produced per month	36kg	43.2 kg
Market Price and Revenue		
Selling price of fresh *danggit*	PhP150 per kg	PhP150 per kg
Selling price of dried *danggit*	PhP1,000 per kg	PhP1,000 per kg
Number of additional laborers		
No. of laborers required	2	0.5-1 (part-time/supervisory)
Monthly total labor wage	PhP2,400	0
Energy consumption and Cost		
Average monthly energy consumption	0 kWh	79.167 kWh
Average monthly energy cost	PhP0	PhP972.17

3.3.2 Projected Annual Financial Operation of Both Types of Drying

Table 6 presents the projected annual financial performance of traditional and IoT-based fish drying systems. The IoT-based dryer exhibits higher annual productivity and sales revenue, driven by year-round operation and reduced drying time. Although automation lowers routine labor requirements, labor-related costs are still incurred for system supervision, maintenance, and operation, and these are reflected in the revised cost structure.

Despite these additional considerations, the IoT-based system maintains higher annual net income due to improved efficiency, reduced drying losses, and increased production capacity. The results confirm that automation does not eliminate labor but reallocates it toward higher-value supervisory and technical tasks, consistent with prior studies on IoT-enabled drying technologies (Hasan *et al.*, 2025; Guanco & Casinillo, 2021).

Table 6. Projected annual financial operation of both types of drying

Indicators	Traditional	IoT-based
Particular	Cost (PhP)	Cost (PhP)
Sales (Benefits)		
Sales – Dried Fish (PhP/yr)	PhP 252, 000	PhP 518,400,00.00
Production Costs		
Cost of Fresh Fish	PhP 189, 000	PhP 388,800.00
Total Wages of Laborers	PhP 16, 800.00	PhP 6,000.00
Other Production Cost		
Material Cost	PhP 2, 000	PhP 11,000.00
Depreciation Expense	PhP 666.67	PhP 3,666.67
Repair and Maintenance	PhP 500	PhP 2,750.00
Interest on Investment Project Cost	PhP 500	PhP 1,100.00
Cost of Energy Consumption	PhP 0	PhP 7, 777.37
Total Annual Production Cost	PhP 209, 166.67	PhP 421, 094.03
ANNUAL NET INCOME	PhP 42, 833.33	PhP 97, 305.97

3.3.4 Financial Viability

The Return on Investment implies that an investor can earn 0.24887 or 24.887 % for every peso invested in the production of dried fish using the IoT-based fish dryer, which is higher than the Traditional sun drying of 0.20478 or 20.478 % only. The Payback period as computed showed that total cost of the IoT-based fish dryer can be recovered in 3.88 years of operation, which is lesser compared to the traditional sun drying of 4.81 years of operation.

3.3.5 Sensitivity Analysis

Table 7 shows that the IoT-based fish dryer remains profitable under all tested conditions. Variations of ±20 % in energy cost and ±25 % in batch load caused only moderate changes in ROI (±6 %), indicating strong resilience to operational cost fluctuations. However, profitability was highly sensitive to dried fish price; a 10 % decrease extended the payback period to over eight years, while a 10 % increase improved ROI to 37.4 %. These findings confirm that the IoT-based fish dryer maintains economic viability across a reasonable range of market uncertainties (Hin *et al.*, 2024).

Table 7. Sensitivity analysis of key economic parameters for the IoT-based fish dryer

Scenario	Dried Fish Price (Php/kg)	Energy Cost (Php/kWh)	Batch size (kg)	ROI (%)	Payback (yr)
Baseline	1000	12.28	2	24.9	3.88
+20% Energy	1000	14.74	2	24.5	4.08
−20% Energy	1000	9.82	2	25.3	3.78
+10% Price	1100	12.28	2	37.4	2.67
−10% Price	900	12.28	2	12.4	8.07
+25% Load	1000	12.28	2.5	31.1	3.22
−25% Load	1000	12.28	1.5	18.7	5.36

3.4 Comparative Technical Description of Traditional and IoT-based Fish Dryer

Table 8 highlights the advantages of the IoT-based fish drying system over traditional methods. The system increases efficiency through automated control, faster drying, and higher drying rates, while maintaining fish quality under hygienic and controlled conditions. Automation reduces labor requirements, and the system operates independently of weather, ensuring consistent production year-round. These factors contribute to higher profitability through increased output, reduced losses, and faster payback. Although the IoT system requires a higher initial investment, it offers a substantially greater return on investment compared to traditional drying methods.

Table 8. Summary of cash inflow and outflow of both types of drying

Indicators	Traditional	IoT-based
Type of Drying System	Manual	Automatic (IoT-assisted)
Hygiene	Low (open)	High (enclosed, controlled)
Monitoring	Manual	Remote and sensored-based
Temperature control	Sun dependent	Automatic control
Weather	Highly dependent	Largely independent
Access to electricity	Not required	required
Ease of use	Simple	Moderately complex
Estimated annual no. of batches	60	240
Fish losses	Prone to spoilage and contamination	Reduced losses
Average drying duration per batch	➢ 2.5 days	~ 3 hours
Average drying rate per batch	~ 6 kg/day	~ 11.5 kg/day
Average drying capacity per batch	15 kg	2 kg
Average drying capacity per month	180 kg	216 kg
Average No. of Workers involved	2	0.5-1 (part-time/supervisory)
Required drying space	Very large	Very small
Quality of dried fish	Acceptable	Improved and consistent
Annual sales benefit	252, 000.00	518,400.00
Annual production cost	209, 166.67	421,094.03
Annual net income	42, 833.33	97,305.97
Annual net cash inflows	43, 500.00	106,972.63
Return on investment	20.478%	24.89%
Payback period	4.808%	3.88%

3.5 Final Product of the IoT-based Fish Dryer

Figure 14 illustrates the appearance of the fish samples after brining and following the drying process using the IoT-based fish dryer, highlighting the physical changes resulting from moisture removal.

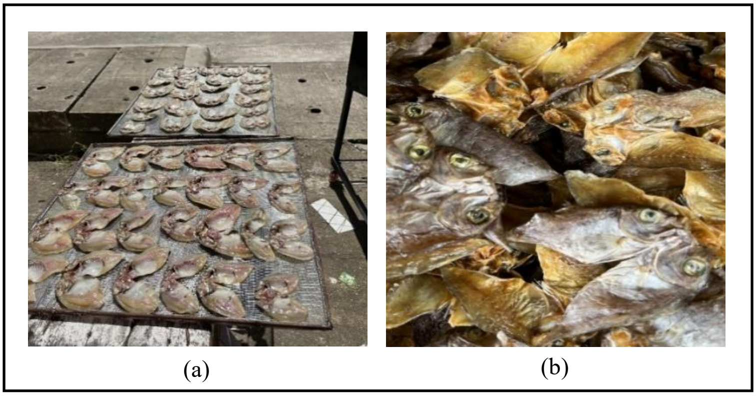

Figure 14. Danggit (*Siganus canaliculatus*) samples: brined (a), dried (b)

4. Conclusion and Recommendation

This study demonstrated that integrating IoT-based monitoring and control into a small-scale fish drying system offers a practical and effective alternative to traditional sun drying for danggit (*Siganus canaliculatus*). Overall, the findings show that the IoT-based dryer provides a controlled, stable, and weather-independent drying environment that addresses the key limitations of conventional sun drying, particularly long drying duration, high dependence on climatic conditions, and inconsistent product quality.

The IoT-based system successfully maintained appropriate thermal and humidity conditions through automated sensing and feedback control, enabling predictable, uniform drying behavior consistent with the established drying kinetics of biological materials. The observed stability of temperature and relative humidity across drying duration and locations indicates an effective system design, ensuring reliable moisture removal while minimizing the risk of spoilage, over-drying, or surface hardening. These characteristics are critical for improving product safety, hygiene, and overall quality in small-scale fish processing.

From an operational and economic perspective, the study indicates that the IoT-based dryer enhances productivity by enabling year-round operation, reducing labor dependence, and shortening processing time. These improvements translate into greater production capacity and improved profitability compared to traditional sun drying, despite the additional energy costs. Sensitivity analysis further suggests that the system remains economically viable under reasonable variations in operating costs, highlighting its resilience to common market and operational uncertainties.

The comparative assessment underscores that while the IoT-based dryer requires higher initial investment and technical complexity, its benefits in terms of efficiency, consistency, hygiene, and economic returns outweigh these limitations. As such, the system presents a viable technology for small fish processors, cooperatives, and rural enterprises seeking to modernize drying practices, reduce postharvest losses, and improve income stability.

Overall, the study contributes to the growing body of evidence supporting the application of IoT-enabled drying technologies in fisheries postharvest processing. It provides a foundation for future work on system optimization, scaling, and integration with renewable energy sources, as well as broader adoption in coastal and rural communities where traditional drying remains prevalent.

5. Acknowledgement

The authors gratefully acknowledge the financial support provided by the University of Eastern Philippines, under the leadership of Dr. Cherry I. Ultra, through the Office of the Vice President for Research, Development, and Extension, headed by Dr. Karina Milagros Cui-Lim. The authors also thank Engr. Kissa Banawis for assistance with statistical analysis and the Barangay Council of Makiwalo, Mondragon, Northern Samar, for logistical support during the conduct of the study.

6. References

Abdinoor, J.A., Hashim, Z.K., Bálint H., Zsebő, S., Stencinger, D., Hegedüs, G., Bede, L., Ijaz, A., & Kulmány, I.M. (2025). Performance of low-cost air temperature sensors and applied calibration techniques: A systematic review. *Atmosphere*, *16*(7), 842–842. https://doi.org/10.3390/atmos16070842

Alvinika, Y., Setyohadi, D.B., & Sulistyoningsih, M. (2021). IoT-based monitoring and design of automatic fish drying equipment using fuzzy logic. IOP Conference

Series: *Earth and Environmental Science, 704*(1), 012042. https://doi.org/10.1088/1755-1315/704/1/012042

Al Kindi, F., Al-Shukaili, T., Pathare, P.B., Al Jahwari, F., Al-Azri, N., & Al Ghadani, O. (2023). Thermal performance of a flat-plate solar collector for drying agricultural crops. *AgriEngineering, 5*(4), 2349–2365. https://doi.org/10.3390/agriengineering5040144

Amigues, L., Pommier-Budinger, V., & Bordeneuve-Guibé, J. (2023). Comparison of control strategies for hysteresis attenuation in electromechanical actuators subject to dispersion. *Control Engineering Practice*, *130*, 105348. https://doi.org/10.1016/j.conengprac.2022.105348

Ampuan, B. (2025). Development of an automatic electric fan. *The Pacific Journal of Science and Technology, 2*(1), 7-11. https://doi.org/10.2139/ssrn.5286246

Ampuan, B., Saldo, K., Espinar, N.A., Olmedo, M.G., Sumayop, R.M., Cu, B.I., & Galon, A. (2026). Development of a microcontroller-based automated pest control spraying system. *Galileo Institute of Technology and Education of the Amazon (ITEGAM) – Journal of Engineering and Technology for Industrial Applications (JETIA), 12*(58), 677–685. https://doi.org/10.5935/jetia.v12i58.2896

Babalis, S.J., & Belessiotis, V.G. (2006). Influence of drying conditions on the drying constants and moisture diffusivity during the thin-layer drying of figs. *Journal of Food Engineering, 65*(3), 449–458. https://doi.org/10.1016/j.jfoodeng.2004.02.005

Bajet, Jr., M.A. (2013). Design and development of fish natural convection drying facility. *JPAIR Multidisciplinary Research*, *12*(1). https://doi.org/10.7719/jpair.v12i1.211

Binici, A., & Kaya, G.K. (2018). Effect of brine and dry salting methods on the physicochemical and microbial quality of chub (*Squalius cephalus* Linnaeus, 1758). *Food Science and Technology*, 38, 66–70. https://doi.org/10.1590/1678-457x.15717

Bureau of Fisheries and Aquatic Resources (BFAR). (2017). Philippine fisheries profile 2017. Department of Agriculture. https://www.bfar.da.gov.ph/wp-content/uploads/2021/05/Philippine-Fisheries-Profile-2017.pdf

Ching, A.A., Luna, M.B., & Ragaza, J.A. (2022). Dried, Salted Fish Products in the Philippines [Review of Dried, Salted Fish Products in the Philippines]. *World Aquaculture*, 60–67.

Chouikhi, H., & Amer, B.M.A. (2023). Performance evaluation of an indirect-mode forced convection solar dryer equipped with a PV/T air collector for drying tomato slices. *Sustainability, 15*(6), 5070. https://doi.org/10.3390/su15065070

Dasin, D.Y., Zakari, A.I., Yahuza, I. (2019). Development of solar energy dryer for fish and meat tested in Modibbo Adama University of Technology Yola. *International Journal of Trend in Scientific Research and Development*, 3(2), 773-777. https://www.ijtsrd.com/papers/ijtsrd21484.pdf

Dasmen, R.N., & Haq, A.D. (2023). Prototype system to anticipate disruption of the IoT-based salted fish drying process. PROtek: *Jurnal Ilmiah Teknik Elektro, 10*(2), 102–106. https://doi.org/10.33387/protk.v10i2.5116

Deef, M., Samy Helal, H., El-Sebaee, I., Nadimi, M., Paliwal, J., & Ibrahim, A. (2023). Harnessing solar energy: A Novel hybrid solar dryer for efficient fish waste processing. *AgriEngineering, 5*(4), 2439–2457. https://doi.org/10.3390/agriengineering5040150

Bureau of Agriculture and Fisheries Product Standards. (2008). Philippine National Standard for dried danggit (PNS/BAFPS 68:2008).

Department of Science and Technology–Food and Nutrition Research Institute (DOST-FNRI) (2020). Philippine food composition table (PhilFCT) online database. https://i.fnri.dost.gov.ph/fct/library

Erbay, Z., & Icier, F. (2010). A review of thin layer drying of foods: Theory, modeling, and experimental results. *Critical Reviews in Food Science and Nutrition, 50*(5), 441–464. https://doi.org/10.1080/10408390802437063

Fernandes, L., & Tavares, P. B. (2024). A review on solar drying devices: Heat transfer, air movement and type of chambers. *Solar, 4*(1), 15–42. https://doi.org/10.3390/solar4010002

Food and Agriculture Organization of the United Nations [FAO]. (2014). Fishery and aquaculture country profiles: The Republic of the Philippines. https://www.fao.org/fishery/facp/PHL/en

Food and Agriculture Organization of the United Nations [FAO]. (2020). The state of world fisheries and aquaculture 2020. https://www.fao.org/state-of-fisheries-aquaculture

Gasco, L., Acuti, G., Bani, P., Dalle Zotte, A., Danieli, P.P., De Angelis, A., Fortina, R., Marino, R., … & Roncarati, A. (2020). Insect and fish by-products as sustainable alternatives to conventional animal proteins in animal nutrition. *Italian Journal of Animal Science, 19*(1), 360–372. https://doi.org/10.1080/1828051x.2020.1743209

Ghafar, H., Wan Rusli, W.A.A., Ismail, M.A., Abdul Nasir, S.M.F., Yamin, A.F., & Yusoff, H. (2025). Implementation of an Internet of Things-based monitoring system to evaluate solar dryer performance on mullet fish. *Food Research, 9*(Suppl. 1), 215-222. https://doi.org/10.26656/fr.2017.9(S1).026

Gilago, M.C., & Chandramohan, V.P. (2022). Performance evaluation of natural and forced convection indirect-type solar dryers during drying ivy gourd: An experimental study. *Renewable Energy*, 182, 934–945. https://doi.org/10.1016/j.renene.2021.11.038

Guanco, J., & Casinillo, L. (2021). Performance Evaluation of a Rice Hull-fueled Cabinet Food Dryer. *Recoletos Multidisciplinary Research Journal, 9*(1), 23–38. https://doi.org/10.32871/rmrj2109.01.03

Hammer, J. (2024). Bang-bang feedback controllers with minimal switching. *International Journal of Control*, 1–16. https://doi.org/10.1080/00207179.2024.2429713

Hasan, N.M., Farhan, N., Aktar, N.S., & Islam, N.K. (2025). Modification and performance evaluation of IoT-enabled solar dryer for fish drying. *GSC Advanced Research and Reviews*, *22*(1), 001-013. https://doi.org/10.30574/gscarr.2025.22.1.0519

Hasan, M.R., Rahman, M.S., & Chowdhury, A.A. (2025). Performance analysis of solar-assisted fish dryers under tropical conditions. *Journal of Food Process Engineering, 48*(2), e14289. https://doi.org/10.1111/jfpe.14289

Hin, L., Buntong, B., Mean, C.M., Chhoem, C., & Prasad, P.V.V. (2024). Impacts of using solar dryers on socio-economic conditions of dried fish processors in Cambodia. *Sustainability, 16*(5), 2130. https://doi.org/10.3390/su16052130

Ilham, D.N., Satria, E., Anugreni, F., Candra, R.A., & Kusumo, H.N.R.A. (2021). Rain Monitoring System for Nutmeg Drying Based on Internet of Things. *Journal of Computer Networks, Architecture, and High-Performance Computing, 3*(1), 52–57. https://doi.org/10.47709/cnahpc.v3i1.933

Institute of Integrated Electrical Engineers of the Philippines (IIEE) (2017). Philippine Electrical Code (Eds). Institute of Integrated Electrical Engineers of the Philippines.

Jasmine, A., & Triawati, E. (2022). IoT-based system for monitoring the drying time of date seeds in the manufacturing of date coffee. *Applied Research and Smart Technology (ARSTech), 3*(1), 1–8. https://doi.org/10.23917/arstech.v3i1.480

Khan, I., Kaur, V.I., & Datta, S.N. (2021). Effect of Fish Silage Supplemented Diets on Growth and Health Status of Pangas Catfish, *Pangasianodon hypophthalm*us Fry. *Indian Journal of Animal Research, 55*(3): 287-294. https://doi.org/10.18805/ijar.b-3954

Kong, D., Wang, Y., Li, M., & Liang, J. (2024). A comprehensive review of hybrid solar dryers integrated with auxiliary energy and units for agricultural products. *Energy*, 293, 130640–130640. https://doi.org/10.1016/j.energy.2024.130640

Luthada-Raswiswi, R., Mukaratirwa, S., & O'Brien, G. (2021). Animal protein sources as a substitute for fishmeal in aquaculture diets: A systematic review and meta-analysis. *Applied Sciences, 11*(9), 3854. https://doi.org/10.3390/app11093854

Mebratu, A.T., Asfaw, Y.T., Merckx, W., Hendriks, W.H., & Janssens G.P.J. (2024). Impact of brining and drying processes on the nutritive value of tambaqui fish (*Colossoma macropomum*). *PLoS ONE 19*(4): e0299926. https://doi.org/10.1371/journal.pone.0299926

Mehta, P., Samaddar, S., Patel, P., Markam, B., & Maiti, S. (2018). Design and performance analysis of a mixed mode tent-type solar dryer for fish-drying in coastal areas. *Solar Energy*, 170, 671–681. https://doi.org/10.1016/j.solener.2018.05.095

Miano, J.I., Nabua, M.A., Gaw, A.R., Alce, A.R.B., Ecleo, C.A.M., Repulle, J.V., & Omar, J.J. (2023). Optimizing drying efficiency through an IoT-based direct solar dryer system: Integration of web data logger and SMS notification. *International Journal of Advanced Computer Science and Applications, 14*(7). https://doi.org/10.14569/IJACSA.2023.0140726

Mishra, N., Jain, S.K., Agrawal, N., Jain, N.K., Wadhwan, N., & N.L. Panwar. (2023). Development of drying system by using internet of things for food quality monitoring and controlling. *Energy Nexus*, 11, 100219–100219. https://doi.org/10.1016/j.nexus.2023.100219

Nnamchi, O.A., Tom, C.N., Akpan, G., Umunna, M.F., Ubong, D., Ibe, M., Linus-Chibuezeh, A., Akuwueke, L., … & Ndukwu, M.C. (2025). Solar dryers: A review of mechanism, methods and critical analysis of transport models applicable in solar drying of product. *Green Energy and Resources*, 100118. https://doi.org/10.1016/j.gerr.2025.100118

Natarajan, S.K., Elangovan, E., Elavarasan, R.M., Balaraman, A., & Sundaram, S. (2022). Review on solar dryers for drying fish, fruits, and vegetables. *Environmental Science and Pollution Research, 29*(27), 40478–40506. https://doi.org/10.1007/s11356-022-19714-w

Oria, C., Palconit, E. (2022). A review on possible combination of solar dryer Materials for Crops in the Philippines. *Engineering and Technology Journal, 07*(07). https://doi.org/10.47191/etj/v7i7.02

Perez, J.H., Andrea, J., Abdu, A., Rosales, M., & Reyes, R. (2024). Performance evaluation of solar-assisted heating system for drying multi-commodity crops. *Mindanao Journal of Science and Technology*, *22*(2). https://doi.org/10.61310/mjst.v22i2.2181

Philippine Atmospheric, Geophysical and Astronomical Services Administration (PAGASA). (2021). Climate of the Philippines. Department of Science and Technology. https://www.pagasa.dost.gov.ph/information/climate-philippines

Philippine Statistics Authority (PSA). (2018). Fisheries statistics of the Philippines, 2018-2020. https://psa.gov.ph/sites/default/files/Fisheries%20Statistics%20of%20the%20Philippines%2C%202018-2020.pdf

Reza, M.S., & Hossain, M.A. (2024). Development and performance assessment of a hybrid solar cabinet dryer for fish drying. *Energy and Thermofluids Engineering*, 3, 29-38. https://doi.org/10.38208/ete.v3.758

Ruzikulov, G., Ibragimov, U., Faiziev, T., Mirzayorova, S., & Ruzikulov, A. (2023). Study of the temperature and humidity regime in solar drying of agricultural products. *BIO Web of Conferences*, *71*, 01042. https://doi.org/10.1051/bioconf/20237101042

Schlünder, E.U. (1988). On the mechanism of the constant drying rate period and its relevance to diffusion controlled catalytic gas phase reactions. *Chemical Engineering Science*, 43(10), 2685–2688. https://doi.org/10.1016/0009-2509(88)80012-5

Shimpy, Kumar, M., & Kumar, A. (2023). Performance Assessment and Modeling Techniques for Domestic Solar Dryers. https://doi.org/10.1007/s12393-023-09335-5

Solanki, J. (2020). Different Types of Fish Drying Methods in Gujarat. *International Journal of Fisheries and Aquatic Studies 2020 [Review of International Journal of Fisheries and Aquatic Studies 2020],* *8*(1), 129–131. https://www.fisheriesjournal.com/archives/2020/vol8issue1/PartB/8-1-24-597.pdf

Southeast Asian Fisheries Development Center. (2022). Fisheries country profile: Philippines. https://www.seafdec.org/fisheries-country-profile-philippines-2022/

Statista (2021). Philippines: Total production volume of fishing 2021. Retrieved from https://www.statista.com/statistics/975932/fisheries-fishing-production-volume-philippines/

Sulzer, M., Christen, A., & Matzarakis, A. (2022). A low-cost sensor network for real-time thermal stress monitoring and communication in occupational contexts. *Sensors, 22*(5), 1828. https://doi.org/10.3390/s22051828

Taide, R., & Deshmukh S.J. (2018). Design, fabrication and performance analysis of a mixed mode solar dryer for drying vegetables. (2018). *International Journal of Latest Trends in Engineering and Technology, 9*(3). https://doi.org/10.21172/1.93.10

Tolentino, L.K.S., Bacaltos, P.C., Cruz, R.M.V., Dela Cruz, N.J.S., Medina, L.R.S., Panergalin, J.V., Padilla, M.V.C., & Velasco, J.S. (2021). Autogation: An alternate wetting and drying-based automatic irrigation and paddy water level control system through Internet of Things. *AGRIVITA Journal of Agricultural Science, 43*(3). https://doi.org/10.17503/agrivita.v43i3.2627

Venkateswarlu, K., Reddy, S.V.K. Recent trends on energy-efficient solar dryers for food and agricultural products drying: a review. *Waste Disposal & Sustainable Energy,* 6, 335–353 (2024). https://doi.org/10.1007/s42768-024-00193-3

Wang, W., Chen, J., Jin, N., Wang, H., Wang, L., & Wu, J. (2024). Thin-layer drying model, drying rate, and effective water diffusion coefficient of pelleted feed. *International Journal of Chemical Engineering*, 2024(1). https://doi.org/10.1155/2024/7092556

Xu, G., & Liu, H. (2025). Efficiency analysis of solar drying system integrated with flat-plate solar collector and thermal storage units. *Renewable Energy, 243*(C), 122569. https://doi.org/10.1016/j.renene.2025.122569

Yang, T., Zheng, X., Xiao, H., Shan, C., & Zhang, J. (2024). Online monitoring system of material moisture content based on the Kalman filter fusion algorithm in air-impingement dryer. *Frontiers in Sustainable Food Systems*, 7. https://doi.org/10.3389/fsufs.2023.1325367

Younis, M.A., Orariath, A.A., Metwally. K.A., Dessoky, E.S., Mahmoud, S.F., Rashed, M.N., Tantawy, A.A., Abdallah, S.E., … & Elwakeel, A.E. (2025). Drying characteristics, environmental and economic analysis of a solar dryer with evacuated tube solar collector for drying Nile tilapia slices. *Scientific Reports, 15*(1), 94194. https://doi.org/10.1038/s41598-025-94194-9

Zhubi-Bakija, F., Bajraktari, G., Bytyçi, I., Mikhailidis, D.P., Henein, M.Y., Latkovskis, G., Rexhaj, Z., Zhubi, E., … & Cicero, A.F.G. (2021). The impact of type of dietary protein, animal versus vegetable, in modifying cardiometabolic risk factors: A position paper from the International Lipid Expert Panel (ILEP). *Clinical Nutrition*, 40(1), 255–276. https://doi.org/10.1016/j.clnu.2020.05.017

Zaboli, M., Seyfolah Saedodin, Mousavi, S., & Karimi, N. (2023). Recent progress on flat plate solar collectors equipped with nanofluid and turbulator: state of the art. *Environmental Science and Pollution Research International*, 30(51), 109921–109954. https://doi.org/10.1007/s11356-023-29815-9